Ab Initio Study of Structure and Bonding of Strontium Clusters

Yixuan Wang,[†] Heinz-Jürgen Flad,*[,‡] and Michael Dolg[§]

Max-Planck-Institut für Physik Komplexer Systeme, Nöthnitzer Strasse 38, D-01187 Dresden, Germany

Received: January 6, 2000; In Final Form: March 23, 2000

Strontium clusters with 2 to 13 atoms have been studied by means of high level quantum chemical ab initio calculations using a scalar-relativistic energy-consistent large-core pseudopotential, a corresponding core-polarization potential, large valence basis sets including up to g functions as well as coupled-cluster and configuration interaction correlation treatments. Equilibrium structures, cohesive energies, vertical as well as adiabatic ionization potentials and electron affinities are reported. Vibrational frequencies for clusters with up to 5 atoms also have been determined. To demonstrate graphically the transition from van der Waals to covalent interactions for increasing cluster size and to comment on the contributions of *sp* and *sd* hybridization to chemical bonding, the electron localization function (ELF) has been calculated from the Hartree−Fock wave functions for the equilibrium structures determined in correlated calculations. Strontium clusters behave rather differently from clusters of the group 12 elements as well as ytterbium, i.e., they exhibit significantly larger cohesive energies than ytterbium clusters due to more pronounced covalent contributions to bonding, and much lower ionization potentials and smaller band gaps. These differences can be mainly attributed to the considerable *sp* as well as *sd* hybridization in strontium clusters, while only either the former or the latter is important for group 12 and ytterbium clusters, respectively.

1. Introduction

During the last two decades there has been considerable interest in the clusters of the divalent elements, i.e., the metals of groups 2 and 12 as well as Yb (see e.g. refs 1, 2 and references therein). These elements are characterized by an s^2 closed-shell ground state configuration and the study of their elemental clusters is motivated principally by several issues. An important reason is that such investigations lead to a better understanding of the transitions in the type of bonding observed for increasing cluster size. The divalent element clusters cover the whole spectrum from the weak van der Waals interactions dominating in small clusters to covalent bonding in medium-sized clusters and finally to metallic bonding for the bulk. The group 12 elements Zn, Cd, and Hg have a completely filled $(n - 1)$d shell, whereas the $(n - 1)$d orbitals are empty in the alkaline earth elements Ca, Sr, and Ba. Similarly, the two mostly divalent lanthanides Eu and Yb may be considered to formally behave as alkaline earth elements, despite the presence of the half-filled 4f shell in Eu. All elements have empty *n*p orbitals which in a polyatomic cluster in principle may form hybrid orbitals with the occupied *n*s valence orbital. The degree of hybridization is related to the magnitude of the energy splittings between *n*s and *n*p, which depend strongly on the position of the specific element in the periodic table, mainly due to shell-structure and relativistic effects. It is very interesting to investigate quantitatively the effect of the different atomic electronic structures on the growth pattern, the chemical bonding as well as other properties of such elemental clusters. Systems with a small number of constituent atoms provide an interesting area of collaboration between experimentalists and ab initio quantum chemists, because the size of the clusters is usually small enough to allow for a very accurate theoretical treatment. The main advantage of ab initio studies over many experimental techniques is that for all calculated properties the conditions under which they should be observed are well defined: one can always specify the electronic states and geometrical arrangements involved, e.g., one can clearly distinguish adiabatic and vertical ionization potentials, etc. A drawback is that it is often unclear how to extract data which can be directly compared to the experimental values. Nevertheless, quantum chemical studies may be used to evaluate, or aid in the design of, new experimental techniques, which in turn might yield useful data for the calibration of the theoretical methods applied. Such a beneficial interplay is certainly also responsible for the recent interest in small to medium-sized clusters.

Quantum chemical ab initio studies of elemental clusters are conveniently performed by means of relativistic pseudopotentials (PP), which restrict the actual calculation to the valence shells and allow the inclusion of relativistic effects in an economical and accurate way. Moreover, since the same valence space can be used for the elements in one group of the periodic table, the PPs allow the treatment of corresponding clusters of different elements on an equal footing. Standard correlation treatments may be applied for the valence electron system, and nonfrozen core effects as well as core-valence correlation effects may be accounted for by adding a core-polarization potential (CPP) to the Hamiltonian. We focused our previous studies in this field first on the transition from van der Waals interactions to covalent type of bonding for Hg clusters with up to 15 atoms.[3,4] Then, bonding was also extensively analyzed for the small clusters M_n $(n = 2-6)$ of Zn and Cd, and compared to those of Hg.[5] The discussion was based on the spectroscopic properties obtained from high level ab initio calculations as well as the

[†] Permanent address: Institute of Theoretical Chemistry, Shandong University, 250 100 Jinan, People's Republic of China.

[‡] Present address: Max-Planck-Institut für Mathematik in den Naturwissenschaften, Inselstrasse 22-26, D-04103 Leipzig, Germany.

[§] Permanent address: Institut für Physikalische und Theoretische Chemie, Universität Bonn, Wegelerstrasse 12, D-53115 Bonn, Germany. E-mail: dolg@thch.uni-bonn.de. FAX: ++49-(0)-228-73-9066.

10.1021/jp000092e CCC: $19.00
Published on Web 05/20/2000

graphical interpretation of the electron localization function (ELF). Finally, we have also examined Yb_n ($n = 2-7$) clusters in order to evaluate the importance of the unfilled 5d orbitals for chemical bonding.[6,7] The necessity to use the medium-core PP(10)+CPP for Yb was demonstrated in contrast to the group 12 clusters, where the large-core PP(2)+CPP works rather well.[8]

In this contribution, we extend our studies to Sr clusters with up to 13 atoms. Sr was chosen since this alkaline earth element often exhibits a relatively large similarity to Yb, the clusters of which we previously investigated.[6] Experimental results for Sr clusters produced in a seeded molecular beam have been published up to Sr_5.[9] The abundance spectrum of small Sr clusters was found to be similar to the one of rare gases, but the magic numbers are different, e.g., for Sr 11 is a magic number, whereas surprisingly 13 is not.[10] On the other hand, 13 is a magic number for the heavier homologue Ba, for reasons that are still unexplained.

Hearn and Johnston[11] investigated Ca and Sr clusters with 2 to 671 atoms using an empirical potential method with two- and three-body interactions. They performed unconstrained geometry optimizations for 2 to 20 atoms and found an icosahedral growth pattern. An enhanced stability was found for 4, 7, 13, and 19 atoms. The authors stated clearly, however, that their model potential, which was derived for the bulk, i.e., adapted to metallic bonding, is likely to fail for small clusters where van der Waals and covalent contributions dominate.

In the framework of electronic structure methods, Sr_2 has been studied with both PP[12] and density functional theory (DFT)[13-15] methods. The former work used a semiempirical PP with two valence electrons augmented by a CPP together with an iteratively selective configuration interaction approach (CIPSI). For ground and excited states of Sr_2 as well as Sr_2^+ the study provided spectroscopic data which agrees favorably with the experimental values. On the other hand, the DFT calculations performed within the local density approximation (LDA) tend to overestimate the strength of bonding in group 2 and 12 clusters significantly, whereas gradient corrections reduce the errors by typically 50%.[14] Recently Qureshi and Kumar[15] investigated the role of 4d orbitals in Sr gas clusters with up to 20 atoms. Within the LDA they applied the PP plane-wave Car−Parrinello (CP) method "ignoring the d states" and the full potential linear muffin-tin orbital (FPLMTO) method treating s, p, and d states on equal footing. In the CP approach the s potential was treated nonlocally, whereas the p potential was used as a local potential, i.e., only s and p orbitals were treated accurately. The authors concluded that the empty Sr 4d orbitals contribute more significantly to the bonding energies as the cluster size grows, expedite the onset of metallicity, and even favor the icosahedral cluster growth pattern. Without d orbitals they obtained maxima in the second derivative $\Delta E_n = E_{n+1} + E_{n-1} - 2\,E_n$ of the binding energy for 4, 7, 10, 15, and 18, whereas the inclusion of d orbitals yielded maxima at 4, 7, 9, 11, 15, 17, and 19. The occurrence of 11 and 19 is in agreement with unpublished experimental evidence,[10] whereas the numbers 10 and 18 obtained without d functions are not. One should note, however, that the calculated binding energy for Sr_2 (0.58 eV) is more than four times larger than the experimental value (0.13 eV). Moreover, the contribution of the d orbitals (0.36 eV) already exceeds the experimental binding energy by almost a factor of 3. Certainly this failure can be attributed to the drawbacks of DFT in the LDA, and in our opinion it limits the validity of the derived conclusions, at least from a quantitative point of view. An unanswered question still remains: how much of the d orbital contribution found by Qureshi and Kumar is real and how much is an artifact, i.e., how large are the uncertainties due to the use of results from two different approaches (CP and FPLMTO without and with d orbitals, respectively) to calculate the binding energy differences. To get an unbiased description of systems where van der Waals and covalent bonding are competing, it is still necessary to use wave function-based ab initio quantum chemical approaches, or alternatively quantum Monte Carlo (QMC) techniques,[4,16] which can equally well describe both types of bonding. Moreover, in contrast to DFT, these two approaches have the merit to be subject to systematic improvements, if needed.

To our knowledge, no other theoretical studies on Sr clusters have been reported in the literature. In the present work we used methods similar to those previously described for the group 12 and Yb clusters.[5,6] The computational results and the analysis of bonding in Sr clusters are compared to our previous findings for the group 12 and Yb clusters in order to shed some light on the effects of sp and sd (and possibly also pd) hybridization on the structure and bonding.

2. Applied Methods and Computational Details

2.1. Pseudopotentials and Basis Sets. In the calculations reported here we have used energy-consistent scalar-relativistic PPs, i.e., medium-core PP(10)[17] and large-core PP(2),[18] together with a core-polarization potential (CPP)[18] for the larger core. PP(10) was only used for Sr_2 in order to calibrate the accuracy of PP(2)+CPP, since a PP(2)+CPP core-definition was found to considerably overestimate the binding energies of Yb clusters. It should be noted that the defects of PP(2)+CPP for Yb are due to the especially low-lying empty Yb 5d orbitals, mainly caused by the incomplete shielding of the nuclear charge by the 4f shell, whereas such a situation is not present for the Sr 4d orbitals. A core−core repulsion correction has been added to the PP(2) valence-only Hamiltonian in order to account for deviations from the point-charge repulsion model between the large Sr^{2+} cores, mainly due to the mutual penetration of the electron densities and the concomitant Pauli repulsion. The use of PP(2)+CPP, in addition to the low computational effort, has the advantage that the basis set superposition error (BSSE) is very small and does not need to be considered.

In the case of PP(10) an uncontracted (9s9p7d5f3g) valence basis set was applied to the atom and Sr_2. To make studies of larger Sr clusters with PP(2)+CPP feasible, a contraction and reduction scheme had to be used for the valence basis set. Starting with an uncontracted (5s5p6d3f1g) set for Sr_n ($n = 2-4$), an uncontracted (5s5p6d1f) set was generated for Sr_n ($n = 5-7$) by simply removing a part of the polarization functions (2f1g), and finally a contracted (5s5p6d1f)/[3s3p3d1f] set was derived for Sr_n ($n = 8-13$) from this primitive set. In calibration calculations for the tetrahedral structure of Sr_4 the smallest basis set yielded a slightly longer bond length (by 0.09 Å) as well as a less than 10% smaller cohesive energy (by 0.037 eV) compared to the largest basis set. No significant change of the ionization potential (increase by 0.01 eV) and electron affinity (decrease by 0.01 eV) was observed. The vibrational frequency was reduced by about 6%. The numerical data concerning the reduction of the valence basis set is listed in Table 1. Unless otherwise noted, the results reported in the following for the atom and the dimer refer to the largest basis set for each PP.

2.2. Correlation Treatment. In general both relativistic and electron correlation effects should be simultaneously taken into account in order to obtain reliable results for systems containing heavy elements. For the systems with several heavy atoms and

TABLE 1: Basis Set Dependence of the Bond Length R_e (Å), Vertical Ionization Potential IP (eV), Electron Affinity EA (eV), Cohesive Energy Per Atom CE (eV), and Totally Symmetric Harmonic Vibrational Frequency ω_e (cm^{-1}) for Sr_4 Using PP(2)+CPP, CCSD(T), and Various Polarized Valence Basis Sets

property	(5s5p6d3f1g)	(5s5p6d1f)	(5s5p6d1f)/[3s3p3d1f]
R_e	4.01	4.04	4.10
IP	4.72	4.72	4.73
EA	0.93	0.92	0.92
CE	0.481	0.457	0.444
ω_e	93.7	91.6	88.2

a large number of electrons compromises with respect to computational feasibility and accuracy have to be made. Relativistic effects are accounted for by PPs, whereas valence electron correlation has to be treated explicitly and is the most costly part of the computations. The single-reference coupled-cluster approach with single and double excitation operators including a perturbative treatment of triple excitations (CCSD-(T)) provides a viable approach for studies of elemental clusters.[4,5] Among the standard ab initio methods the CCSD-(T) method is, for cases dominated by a single Hartree−Fock (HF) reference configuration, the one which permits the most accurate treatment of electron correlation. Furthermore, it is strictly size-extensive, which is of fundamental importance for studies of the size-dependence of cluster properties. However, to go beyond Sr_9, less costly correlation treatments such as configuration interaction with single and double excitations, including the Siegbahn size-extensivity correction (CI(SD)+SEC), had to be applied. The HF, CI(SD) and CCSD(T) calculations reported here were performed with the MOLPRO program package.[19]

2.3. Electron Localization Function (ELF). Becke and Edgecombe[20] developed the so-called electron localization function (ELF) as a measure for the probability of finding an electron in the neighborhood of another electron with the same spin. By its construction ELF may adopt values between zero and one. A large value of ELF means that the reference electron is highly localized, i.e., the probability of finding a second electron with the same spin near the reference point is low. Regions which are usually associated with covalent bonds, lone pairs, or inert cores exhibit high ELF values. In contrast, low ELF values are typical for the regions between electronic shells, and regions where van der Waals interactions dominate. Although ELF is also defined for very low electron densities, its values in these regions are not meaningful for chemical bonding. The interpretation of ELF should be done inside the 0.001 au isosurface of the electron density, which corresponds approximately to the van der Waals "size" of the system. In all ELF plots presented in this work, the outermost contour line corresponds to this value of the electron density. We also used the medium-core PP(10) instead of the large-core PP(2), to account for effects of the core−electron density. ELF was extensively applied to various molecules, clusters, and solids[5,21] and yielded meaningful, easily understandable, and visually directive patterns of the interactions between vicinal atoms. However, as already pointed out previously,[6] care has to be taken when the characteristic 2D sections are selected, especially when directional bonding occurs and "strained" bonds are present. The characteristic maxima (or minima) of ELF in polyatomic systems might not always be located on straight lines interconnecting two atoms or in planes defined by three atoms. For the evaluation of ELF a separate program[22] was interfaced to the MOLPRO code.[19]

TABLE 2: First and Second Ionization Potentials IP_i ($i = 1,2$) (eV) and Dipole Polarizability α (a.u.) of Sr Using Pseudopotentials with Different Core Definitions

methods	IP_1	IP_2	α
PP(2)+SCF	4.75	10.47	231.7
PP(2)+CI	5.51	*a*	229.8
PP(2)+CPP+SCF	5.09	11.02	189.0
PP(2)+CPP+CI	5.71	*a*	202.3
PP(10)+SCF	4.75	10.44	233.0
PP(10)+CCSD(T)	5.66	10.97	200.0
exp	5.70	11.03[b]	186 ± 15[c],192[d]

[a] Identical to SCF result. [b] Ref 12. [c] Ref 36. [d] Ref 37. Basis sets: (5s5p6d3f1g) for PP(2), (9s9p7d5f3g) for PP(10).

It was argued in a previous paper on Yb clusters[6] that although ELF is based on the Hartree−Fock wave function and does not take into account electron correlation explicitly, it accounts for those effects indirectly, as long as it is evaluated at the equilibrium structures derived from correlated, e.g., CCSD(T), calculations. Covalent contributions to bonding can also be defined in terms of charge fluctuations.[23] It was found that for the group 12 dimers the analysis of such contributions in terms of correlated and uncorrelated charge fluctuations parallels the one using ELF.[5] The dominant bonding contribution in these systems comes from the van der Waals interactions, i.e., a pure correlation contribution which does influence the equilibrium bond lengths considerably, but does not affect the charge fluctuations. The covalent contributions are already largely accounted for in the Hartree−Fock wave function, a fact which is exploited in a newly designed hybrid model for the study of large Hg clusters.[8] Charge fluctuations were in fact found to be quite insensitive with respect to electron correlation.[8,27] Therefore it seems to be justified for the evaluation of ELF to take electron correlation only indirectly into account via the optimized structures.

3. Results and Discussion

3.1. Sr, Sr_2, Sr_2^+. Before discussing larger Sr clusters, it is necessary to investigate the first and second ionization potential and the dipole polarizability of the neutral Sr atom, as well as the spectroscopic properties of Sr_2 and Sr_2^+, to check the accuracy of the applied methods by a comparison to available experimental data. Note that the first ionization potential as well as the dipole polarizability occur in the approximation to the London formula for van der Waals interactions, i.e.,

$$\Delta E^{\mathrm{disp}} = -3\, IP_1\, \alpha^2/(4\, R^6) \qquad (1)$$

The results of these calibration calculations are summarized in Tables 2 and 3.

In the atomic calculations (Table 2) PP(2) and PP(10) yield very similar results at the SCF level, i.e., frozen core errors due to the large Sr^{2+} core of PP(2) appear to be small. At the CI level a significant difference occurs for IP_1, which is mainly due to the neglect of core-valence correlation effects in calculations with PP(2). Accounting for these by adding a CPP, the CI results of PP(2)+CPP and the CCSD(T) results of PP-(10) are in very close agreement, the former ones being even a bit closer to the experimental values, probably due to an incomplete account for explicit core-valence correlation contributions in the PP(10) work.

Previous experience shows that large-core PPs tend to result in a too short bond distance and a too large binding energy, especially when unoccupied shells with higher angular quantum number and lower main quantum number than the actual valence

TABLE 3: Bond Length R_e (Å), Vertical Ionization Potential IP_v (eV), Adiabatic Ionization Potential IP_a (eV), Cohesive Energy per Atom CE (eV), and Harmonic Vibrational Frequency ω_e (cm^{-1}) for Sr_2 and Sr_2^+ from CCSD(T) Calculations Using PP(2)+CPP and PP(10)

	Sr_2			Sr_2^+		
	PP(2)	PP(10)	exp.[a]	PP(2)	PP(10)	exp.[b]
R_e	4.60	4.72	4.45	4.12	4.20	
IP_a	4.71	4.73	4.737 ± 0.012			
IP_v	4.80	4.83				
CE	0.066	0.065	0.066 ± 0.002	0.565	0.53	0.546 ± 0.0081
ω_e	41.5	39.1	40.32 ± 0.02	82.3	80.6	86 ± 3

[a] Ref 28. [b] Ref 9. Basis sets: (5s5p6d3f1g) for PP(2), (9s9p7d5f3g) for PP(10).

orbitals are present.[24−26] Although atomic data for the valence states is reproduced with good accuracy, molecular results may be in error. The results listed in Table 3 indicate that Sr behaves completely different from Yb. The bond length, cohesive energy as well as vibrational frequency of Sr_2 and Sr_2^+ obtained with the two approaches are in quite good agreement. Moreover, the results for PP(2)+CPP (R_e = 4.60 Å, D_e = 0.132 eV, ω_e = 41.5 cm^{-1}) are even in slightly better agreement with the experimental values (R_e = 4.45 Å, D_e = 0.132 ± 0.004 eV, ω_e = 40.3 cm^{-1})[28] than those of PP(10) (R_e = 4.72 Å, D_e = 0.130 eV, ω_e = 39.1 cm^{-1}). Since a smaller PP core usually is the more accurate approach, this is probably due to an incomplete treatment of electron correlation, especially core-valence correlation, in the case of PP(10). Hence, in terms of the achievable accuracy as well as with respect to the computational savings PP(2)+CPP appears to be more suitable for the investigation of Sr_n clusters. Excellent agreement is also obtained with the results of Boutassetta et al.,[12] who used the same PP, but a different formulation of the CPP and a smaller basis set including only up to one f function (R_e = 4.53 Å, D_e = 0.135 eV, ω_e = 43.0 cm^{-1}).

To investigate the importance of p and d orbitals to bonding in Sr_2 we performed calculations with PP(2)+CPP and (5s5p), (5s6d) and (5s5p6d) basis sets. The CCSD(T) results for (5s5p) (R_e = 6.20 Å, D_e = 0.012 eV, ω_e = 9.4 cm^{-1}) as well as for (5s6d) (R_e = 5.75 Å, D_e = 0.010 eV, ω_e = 9.4 cm^{-1}) are both considerably worse than for (5s5p6d) (R_e = 4.73 Å, D_e = 0.091 eV, ω_e = 33.4 cm^{-1}). Neither p nor d functions alone are able to bring the results into acceptable agreement with the experimental numbers, and the comparison of the (5s5p6d) results to those of (5s5p6d3f1g) discussed in the last section reveals that f and g orbitals make a nonnegligible contribution to bonding. Looking at Sr_2 at the PP(2)+CPP CCSD(T) equilibrium distance, we find that the difference of the binding energies derived from (5s) and (5s5p6d) is 50.2% a SCF effect and 49.8% a correlation effect. The SCF contributions of p and d functions are 58% and 48%, if added to the (5s) set, or 52% and 42% if deleted from the (5s5p6d) set, i.e., p and d orbitals are of equal importance. The corresponding correlation contributions of p and d functions behave less additive, i.e., 19% and 56% for addition to the (5s) set, or 44% and 81% for deletion from the (5s5p6d) set. Since SCF does not account for the van der Waals interactions, we can state that p and d functions make almost equal covalent contributions to bonding in Sr_2. More difficult is the analysis of the correlation part, which describes the van der Waals interactions but also correlation corrections to the covalency. If we assume that the van der Waals contributions are well described by the approximate London formula given above, then only a small d orbital participation is expected: the dipole polarizability for the (5s6d) set equals the Sr^{2+} core polarizability of the CPP (5.1 au) due to symmetry reasons, i.e., s → p excitations mixing in the spherical symmetric ground state s^2 configuration cannot occur and only the polarizability accounted for by the Hamiltonian contributes, whereas the (5s5p) set accounts for roughly 99% and 73% of the SCF (189.0 au) and CI (202.3 au) basis set limits, respectively. No contributions to IP_1 arise at the SCF level, but the error with respect to the CI basis set limit is 0.35 and 0.07 eV for the (5s6d) and (5s5p) sets, respectively. Finally the (5s5p6d) set yields results in almost perfect agreement with the CI basis set limits, i.e., 99% of the dipole polarizability are recovered and the error in IP_1 is 0.01 eV. This indicates that the correlation contribution of the d orbitals in Sr_2 is mainly of covalent character, less of van der Waals character.

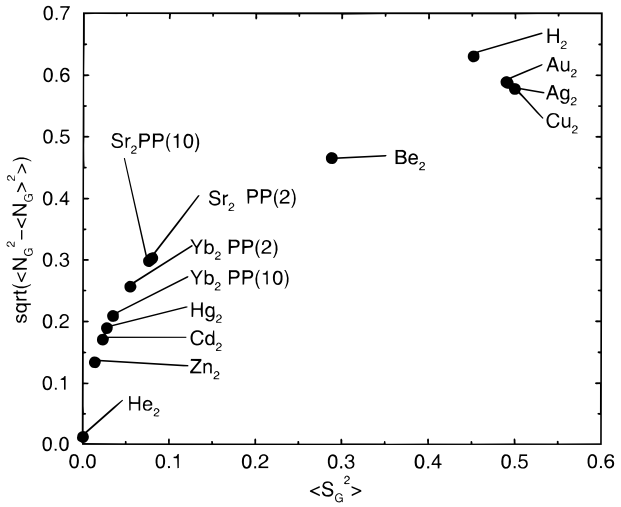

Figure 1. Charge fluctuations $(\langle \delta N^2 \rangle)^{1/2}$ and square of the local spin $\langle S^2 \rangle$ for *n*s and *n*p localized valence orbitals on one of the two atoms of M_2 (M = H, He, Be, Cu, Zn, Sr, Ag, Cd, Yb, Au, Hg). The limiting value of the charge fluctuation is 0.707 for a covalent single bond, whereas a pure van der Waals interaction corresponds to a value of zero. The value of the square of the local spin on each of the separated atoms is zero for S = 0 and 0.866 for S = 1/2.

In the case of the Sr_2 ground state, we still want to address the question of covalent bonding contributions besides the dominant van der Waals interactions. Similar to the previous studies of the group 12 dimers[29] and Yb_2,[7] we assume that the major covalent contributions, if present, could be treated at the CASSCF level with a "5s and 5p" active orbital space and would result in nonzero charge fluctuations $(\langle \delta N^2 \rangle)^{1/2}$, where N denotes the occupation number operator for a subset of the four orbitals localized on one of the two atoms. It should be noted that the active orbital space also contains admixtures of d, f, and g functions and the notation "5s and 5p" is a formal one. The charge fluctuations and the square of the local spin $\langle S^2 \rangle$ on one atom are compared to corresponding results for Be_2, the group 12 dimers and Yb_2 in Figure 1. The group 11 dimers exhibit a single essentially covalent bond and are included for comparison to the mainly van der Waals bonded group 12 dimers. H_2 and He_2 have also been included as limiting cases for a single covalent bond and a pure van der Waals interaction, respectively. In contrast to Yb_2, nearly the same charge fluctuation and local spin on Sr are observed for PP(2)+CPP and PP(10) in case of Sr_2. The plots of the charge fluctuation against the square of the local spin $\langle S^2 \rangle$ indicate that the covalent contributions to bonding are somewhat stronger in Sr_2 than in Yb_2 and the group 12 dimers, but they are much smaller than in Be_2, where a significant local spin on each Be atom is observed.

3.2. Structures and Cohesive Energies. The number of possible Sr cluster structures increases very rapidly with the number of atoms, even when only closed-shell ground states are considered. The best approach would be an unconstrained structure optimization, e.g., the simulated annealing method or molecular dynamics, based on a high quality ab initio treatment for the electronic energy, e.g., CCSD(T). The large number of minima to be searched in order to find the global minimum as well as the high computational cost of each ab initio step renders such an optimization procedure impracticable. Essentially two ways to circumvent these problems exist. Most of the work reported in the literature on the group 2 elements uses a cheaper, and also less accurate, method for the evaluation of the electronic energy, namely DFT[15,30−32] or effective many-body potentials[11] adjusted to solid state properties. We chose the alternative to apply highly accurate electronic structure methods, but we restricted the search for the global energy minimum to the most likely structures. Our main motivation is that we are interested in the transition from van der Waals to covalent bonding for clusters with a relatively small number of atoms, where only a few structures are good candidates for the global minimum. Since present-day DFT does not provide functionals which are able to describe accurately van der Waals interactions, and model potentials adjusted to the bulk metal are also not appropriate for this purpose, only wave function-based ab initio methods remain as suitable tools.

Based on the assumption of predominantly van der Waals bonding in small Sr clusters those structures seem to be especially favorable which allow a dense packing of the atoms and maximize the number of nearest neighbor interactions. Therefore, we have considered in our work only regular and compact structures which fulfill these requirements, i.e., equilateral triangular ($n = 3$), tetrahedral ($n = 4$), trigonal bipyramidal and quadrilateral pyramidal ($n = 5$), octahedral and bicapped tetrahedral ($n = 6$), as well as pentagonal bipyramidal, capped octahedral and bicapped trigonal bipyramidal ($n = 7$) structures. From Sr_8 onward, only a singly or multiply capped pentagonal bipyramidal structure was considered until the icosahedron for Sr_{13} was reached.

Since the photoelectron spectra (PES) of negatively charged clusters are used to determine the band gap,[33] and most likely significant differences exist between the equilibrium geometries of the neutral and the charged clusters, the equilibrium geometries of negatively and positively charged Sr_3 and Sr_4 were also located. The structures have been optimized within a given symmetry using the CCSD(T) and/or CI(SD) method. To ensure that the determined structures are real minima a normal coordinate analysis has been performed.

Our results are summarized in Tables 4 ($Sr_3 - Sr_5$), 5 ($Sr_6 - Sr_8$) and 6($Sr_9 - Sr_{13}$). The calculated properties include bond lengths (R_e), cohesive energies per atom (CE), vertical ionization potentials (IP) and electron affinities (EA). The harmonic vibrational frequencies ω obtained from a normal coordinate analysis are given for Sr_3, Sr_4, and Sr_5.

For Sr_3 and Sr_3^- the equilateral triangular geometries are found to have by 0.55 and 0.40 eV, respectively, lower energies than the corresponding linear ones. The bond length of the negatively charged cluster (4.03 Å) is slightly (by ~0.13 Å) shorter than the neutral one (4.16 Å). For Sr_3^+ a linear geometry (4.19 Å) was found to be only 0.11 eV lower in energy than the triangular one. The difference between the adiabatic (4.62 eV) and vertical (4.72 eV) IP of Sr_3 is far less pronounced than for the corresponding group 12 clusters, e.g., 6.85 eV vs 7.93 eV for Cd_3.[5] In the case of the tetrahedral geometries the bond lengths of Sr_4^+ (4.02 Å) as well as Sr_4^- (4.01 Å) are very close to the one of the neutral system Sr_4 (4.01 Å). The singly occupied orbital of Sr_4^+ falls in the t_2 irreducible representation of T_d symmetry and therefore Sr_4^+ is subject to a Jahn−Teller distortion. We found the $^2A_1$ state to be lowest in energy in C_{2v} symmetry. The equilibrium structure is essentially that of a tetrahedron compressed in the direction of the C_2 axis. Four interatomic distances are slightly shorter (3.95 Å) than for the tetrahedral structure, whereas two are significantly longer (4.39 Å). The adiabatic IP of Sr_4 (4.60 eV) is 0.12 eV lower than the vertical IP (4.72 eV).

Similar to Sr_2 we investigated Sr_4 with respect to the importance of p and d functions. The results for the (5s5p) ($R_e = 4.89$ Å, CE = 0.05 eV), (5s6d) ($R_e = 4.29$ Å, CE = 0.15 eV) and (5s5p6d) ($R_e = 4.05$ Å, CE = 0.39 eV) basis sets again indicate that both p and d functions are important to get results near to the best CCSD(T) values ($R_e = 4.01$ Å, CE = 0.48 eV), also this mutual dependence is smaller than for Sr_2. At the PP(2)+CPP CCSD(T) equilibrium distance, we find that the difference of the binding energies derived from (5s) and

TABLE 4: Bond Length R_e (Å), Vertical Ionization Potential IP_v (eV), Adiabatic Ionization Potential IP_a (eV), Electron Affinity EA (eV), Cohesive Energy per Atom CE (eV), and Harmonic Vibrational Frequency ω_e (cm^{-1}) for Sr_n ($n = 3,4,5$) from CCSD(T) Calculations

	Sr_3	Sr_4	Sr_5	
	D_{3h}	T_d	D_{3h}	C_{4v}
R_e	4.16	4.01	3.96,4.07[a]	4.25,4.10[a]
IP_v	4.72	4.72	4.09	3.83
IP_a	4.62	4.60		
EA	0.887	0.93	0.90	1.34
CE	0.245	0.481	0.512	0.368
ω_e	71.9(A'_1)	61.8(E)	98.9,57.1(A'_1)	
	63.9(E')	76.4(T_2)	81.8,47.7(E')	
		91.6(A_1)	78.1(A''_2)	
			59.4(E'')	

[a] The bond lengths refer to equatorial and axial bonds, respectively; basis sets: (5s5p6d3f1 g) for Sr_3 and Sr_4, (5s5p6d1f) for Sr_5.

TABLE 5: As Table 4, but for Sr_n ($n = 6, 7, 8$)[a]

	Sr_6		Sr_7	Sr_8
	C_{2v}	O_h	D_{5h}	C_s
R_e	4.02,4.12[b]	3.94	4.14,4.02[c]	4.19,4.08,4.15[d](4.21,4.10,4.12)
IP	4.08	3.86	4.18	4.02(3.92)
EA	1.07	1.24	0.99	1.05(0.99)
CE	0.553	0.447	0.680	0.688(0.540)

[a] The values in parentheses refer to CI(SD)+SEC instead of CCSD(T). [b] The bond lengths refer to an edge of the tetrahedron and the distance between a cap atom and a tetrahedral atom, respectively. [c] The bond lengths refer to equatorial and axial bonds, respectively. [d] The bond lengths refer to equatorial, axial bonds and the distance between a cap atom and a surface atom of a pentagonal bipyramid. Basis sets: (5s5p6d1f) for Sr_6 and Sr_7, (5s5p6d1f)/[3s3p3d1f] for Sr_8.

TABLE 6: As Table 4, but for Sr_n ($n = 9-13$). CI(SD)+SEC was used instead of CCSD(T)

	Sr_9	Sr_{10}	Sr_{11}	Sr_{12}	Sr_{13}
R_e	4.18,4.06, 4.13[a]	4.18,4.06, 4.18[a]	4.18,4.05, 4.14[a]	4.19,4.06, 4.13[a]	4.27
IP	3.65	3.43	3.38	3.37	3.37
EA	0.99	0.972	1.08	1.09	1.08
CE	0.587	0.590	0.605	0.620	0.636

[a] The bond lengths refer to equatorial, axial bonds and the distance between a cap atom and a surface atom of a pentagonal bipyramid. Basis set: (5s5p6d1f)/[3s3p3d1f].

(5s5p6d) is 64.6% a SCF effect and 35.4% a correlation effect. Probably this bias toward the SCF contributions reflects the decreasing importance of van der Waals contributions in Sr_4 compared to Sr_2. The SCF contributions of p and d functions are 58% and 65%, if added to the (5s) set, or 35% and 42% if deleted from the (5s5p6d) set. When comparing these numbers to the ones for Sr_2 one may speculate about a slight increase of the importance of d functions with respect to p functions. This is supported by a Mulliken analysis: 3.4% and 1.1% of the charge are in the p and d orbitals for Sr_2, whereas the corresponding values are 11.5% and 7.1% for Sr_4. In contrast to Sr_2 the corresponding correlation contributions of p and d functions behave almost additive for Sr_4, i.e., 22% and 80% for addition to the (5s) set, or 20% and 78% for deletion from the (5s5p6d) set. The d functions are here definitely more important than the p functions.

The calculated trigonal bipyramid (D_{3h}) and quadrilateral pyramid (C_{4v}) of Sr_5 each have two types of atoms, axial and equatorial and "peak" and "base", respectively, leading to two types of bonds. The equatorial bond for the D_{3h} geometry is shorter by 0.11 Å than the axial bond, which can be attributed to the different number of nearest-neighbor interactions for the peak and base atoms. In the case of the C_{4v} structure the peak-to-base bond length is shorter than the base-to-base bond length by 0.15 Å. It turns out that the D_{3h} structure is 0.72 eV lower in energy than the C_{4v} structure, and has a slightly shorter averaged bond length (by $\approx$ 0.15 Å). This is similar to previous findings for Hg_5 and Yb_5.[5,6]

In the case of the octahedral geometry of Sr_6, like in the PP-(2)+CPP calculations of Yb_6,[6] the ground state does not result from the expected $a_{1g}^2\ t_{1u}^6\ e_g^4$ valence orbital configuration, but rather from $a_{1g}^2\ t_{1u}^6\ e_g^2\ a_{1g}^2$. From the three possible states $^3A_{2g}$, ^1E_g, and $^1A_{1g}$ we find the $^3A_{2g}$ state to be lowest in energy. The first excited state is ^1E_g, and the triplet−singlet splitting derived from multireference averaged coupled-pair functional (MRACPF) calculations amounts to 0.23 eV. We note that, in contrast to the previous investigation of Yb_6,[6] the ordering of the electronic states obtained with PP(2)+CPP was also confirmed with the presumably more accurate PP(10). Again, this demonstrates that PP(2)+CPP is a reasonable choice for investigating Sr clusters. Another point which should be mentioned for Sr_6 is that the lowest energy structure obtained from the many-body potential[11] as well as the LDA[15] approaches is the octahedral structure, but the present CCSD(T) study indicates that a bicapped tetrahedral structure of Sr_6 with a singlet state occurs to be more stable than the octahedral one with a triplet state by 0.636 eV. Nevertheless, the averaged bond length of the bicapped tetrahedral structure (4.07 Å) is significantly larger than of the octahedral one (3.94 Å). The bond lengths in the tetrahedral skeleton agree quite well with those of Sr_4, i.e., 4.02 vs 4.01 Å. Similar results have been obtained previously for the homologues of the group 12 and Yb. The results for the triplet state of the octahedral structure and the singlet state of the bicapped tetrahedral structure are listed in Table 5.

For Sr_7 the CI(SD)+SEC calculations for the three kinds of geometries indicate that the pentagonal bipyramid (D_{5h}) has the lowest energy. The bicapped trigonal bipyramid is 0.54 eV, and the capped octahedron higher in energy at 0.83 eV. The pentagonal bipyramidal structure was further optimized at the CCSD(T) level. The equatorial bond length (4.14 Å) is slightly larger than the axial bond length (4.02 Å) by approximately 0.12 Å, while the distance between the two axial atoms (3.88 Å) is significantly shorter than the latter by about 0.26 Å.

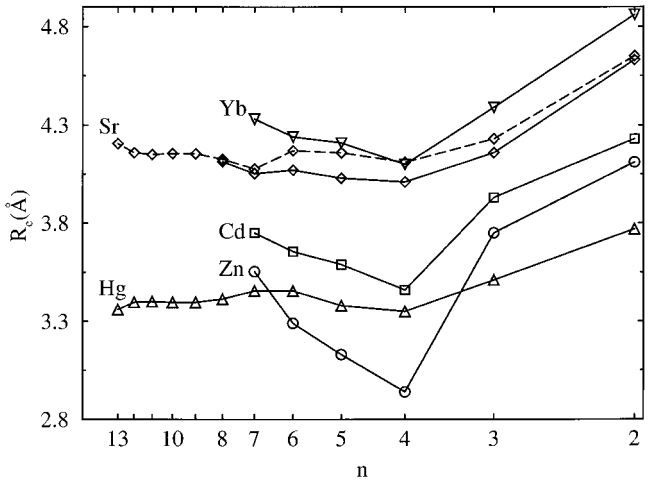

Figure 2. Averaged nearest-neighbor bond lengths $\bar{R}_e$ (Å) in Sr ◇, Yb ▽, Zn ○, Cd □, and Hg △. The solid and dashed lines refer to the Sr_n CCSD(T) and CI(SD)+SEC results, respectively.

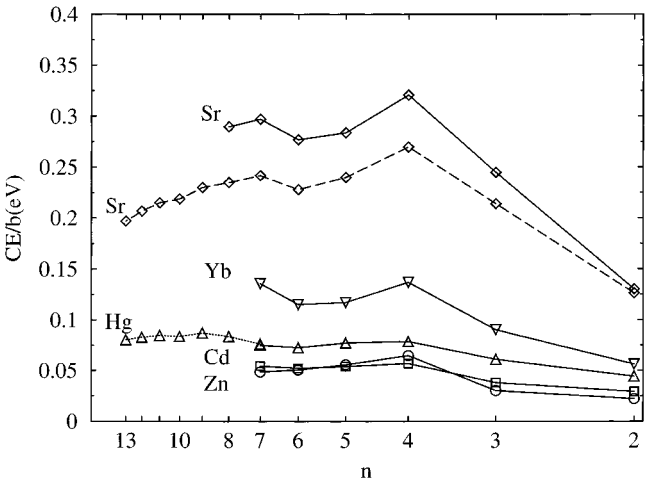

Figure 3. Dissociation energies per nearest neighbor interaction CE/b (eV). The symbols have the same meaning as in Figure 2. The dotted line for Hg denotes PDMC results from ref 4.

Based on the findings for the lowest energy structure of Sr_7, it seems reasonable to assume that Sr_8 and other larger clusters can be formed by capping the pentagonal bipyramid faces with additional atoms, and finally arrive at the icosahedral geometry for Sr_{13}. The FPLMTO[15] and many-body potential methods[11] also found that the lowest energy isomers for these clusters have a icosahedral geometry. The CI(SD)+SEC calculations show that the lengths for the three kinds of bonds stay almost constant from Sr_8 to Sr_{12}, while the cohesive energies are slightly increased.

The size-dependence of the averaged bond length $\bar{R}_e$ and the cohesive energy per nearest-neighbor interaction (CE/*b*) are shown in Figures 2 and 3, respectively. Only the most stable structures are included for those cases where two or more structures were calculated. For comparison we have also shown the corresponding results for the group 12 and Yb clusters. The number of nearest neighbor interactions may be found by inspection of the structure for simple cases, e.g., small clusters, but it may be more difficult to establish uniquely for larger systems. We looked at the distribution of interatomic distances for the clusters with 7 to 13 atoms and found a gap with no values between 4.7 and 6.5 Å. Therefore we considered only the pairs of atoms with distances below 4.7 Å for the nearest-neighbor interactions. Their number for the clusters with 2 to 13 atoms are 1, 3, 6, 9, 12, 16, 19, 23, 27, 31, 36, and 42. The

same numbers have been found for the Hg clusters. Again, in the distribution of the interatomic distances of the more complicated structures with 7 to 13 atoms we found a gap without values between 3.8 and 5.4 Å. The averaged bond length curves for Sr clusters from CCSD(T) as well as CI(SD)+SEC exhibit two clear local minima at $n = 4$ and to a lesser extent at $n = 7$, which correspond to local maxima in the CE/*b* curves. This result indicates an exceptional stability of the tetrahedral and pentagonal bipyramid structures, in agreement with the experimental evidence that 4 and 7 are the lowest magic numbers for Sr clusters.[10] From Sr_7 to Sr_{13}, the CE/*b* values decrease slowly and monotonically, which is consistent with the fact that, surprisingly, Sr_{13} has not been found to be especially stable in experiment. The averaged bond length values increase from Sr_7 to Sr_{13}, with a plateau, or actually a very shallow minimum, around Sr_{11}. Although we cannot find a cluster between $n = 8$ and $n = 13$ which has a pronounced higher stability than its neighbors, we note that experimentally $n = 11$ has been found to be a magic cluster size. In general Sr clusters have slightly shorter bonds than the Yb clusters, but considerably longer bonds than the corresponding group 12 clusters. Their CE/*b* values are significantly higher than for Yb clusters as well as for the group 12 clusters. Nevertheless, the trend in CE/*b* with increasing cluster size appears to be qualitatively quite similar for Sr and Yb, e.g., local maxima appear at $n = 4$ and $n = 7$. This again indicates larger covalent bonding contributions in Sr clusters compared to their Yb and group 12 homologues, cf. also Figure 1 for the dimers.

The dipole polarizability of the group 2 and 12 elements and of Yb increases in the order Be,Zn,Hg < Cd < Mg < Ca,Yb < Sr < Ba, the first ionization potential as Ba < Sr < Ca,Yb < Mg < Cd < Be,Zn < Hg and the bond distance in the homonuclear dimers as Be < Hg < Mg,Zn,Cd < Ca,Yb < Sr,Ba. The ratios between the largest and smallest value are roughly 8, 2, and 2 for the dipole polarizability, the first ionization potential, and the atomic radius, respectively. Since the dipole polarizability enters quadratically in the London formula and the interatomic distance reciprocally with the sixth power, these two quantities are much more important for estimating the strength of van der Waals interactions than the ionization potential. Using the London formula the strength of the van der Waals bond in the homonuclear diatomics should increase as Zn < Cd,Hg < Mg < Ca,Sr,Yb < Ba < Be, whereas the actual binding energies increase as Zn,Cd,Hg < Mg < Be < Ca < Sr < Yb < Ba. We note here in passing that these orderings are not strict, since in some cases there is a lack of accurate experimental data or no experimental data at all. Leaving aside the special case of Be_2,[34] one observes that the actual ordering of the binding energies is roughly predicted by the London formula. The reason is that the covalent contributions to bonding, cf. Figure 1, obey essentially the same trend as the van der Waals contributions predicted by the London formula. In our opinion is not possible to estimate the strength of bonding in the larger group 2, 12 or Yb metal clusters exclusively on the basis of atomic and diatomic data, e.g., Sr and Yb clusters, according to all that was discussed above, should behave very similarly, however already when going from the dimer to the trimer a large difference in the cohesive energy is observed (Figure 2).

3.3. Ionization Potentials, Electron Affinities, and Band Gap. Vertical ionization potentials (IP) and electron affinities (EA) of Sr_n have been calculated by CCSD(T) and CI(SD)+SEC for $n \leq 8$ and only CI(SD)+SEC for $n > 8$. The size-dependence of IP is presented in Figure 4. The results for group 12 and Yb clusters are also included. The changes of the IP with cluster size for Sr, Yb, and Hg are very similar, at least up to 7 atoms, i.e., IPs gradually decrease from 2 to 4, significantly decrease from 4 to 5, and then gradually decrease again. IP values for Sr clusters are slightly lower than those of the Yb clusters (by ~0.5 eV) and are much lower than those of the group 12 clusters (by ~1.5−2.0 eV). The behavior of the IP provides no indication for the completely different evolution of covalency in the clusters of these elements. Beyond that, as in the cases of group 12 and Yb clusters, the IPs of different structures of the same cluster size are also rather similar. For instance, this can be observed for the D_{3h} bipyramid and the C_{4v} pyramid for Sr_5 where the difference is 0.26 eV and only 0.22 eV for the octahedral and bicapped tetrahedral structure for Sr_6. Figure 4 also shows that the IPs from CCSD(T) and CI(SD) are in good agreement, although the quality of the basis set for the CI(SD) calculation is considerably reduced and the electron correlation treatment is less accurate.

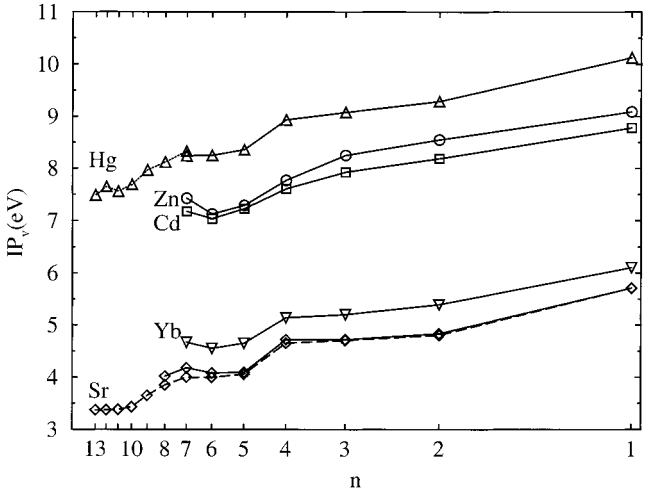

Figure 4. Vertical ionization potentials IP (eV) for Sr, Yb, and the corresponding group 12 clusters. The symbols have the same meaning as in Figure 2. The dotted line for Hg denotes PDMC results from ref 4.

We also observed that less stable structures sometimes have somewhat larger vertical electron affinities, for instance, the EAs are 0.90 and 1.34 eV for the D_{3h} and C_{4v} structures of Sr_5, respectively. This means that such less stable structures of the neutral clusters should also be considered when comparing calculated EAs with those derived from the photoelectron experiments for the vertical ionization of negatively charged clusters.[33] In contrast to the behavior observed for small Hg clusters, where the correlation contribution to the IP decreases rapidly and disappears for Hg_4, it remains approximately constant at a value of 0.5 eV for the Sr clusters. This is similar to the Yb case, where electron correlation effects remain constant at about 0.3 eV.

More interesting than the individual properties IP and EA is their difference BG = IP − EA shown in Figure 5. In solids BG is identical to the band gap and in a one-particle picture it corresponds to the splitting between the highest occupied and the lowest unoccupied orbitals (molecules, clusters) or Bloch functions (polymers, solids). We adopt the definition BG = IP − EA for clusters in order to go beyond the one-particle picture, i.e., to include electron correlation effects. For the clusters one has a predominant van der Waals interaction for the dimers (BG ≫ 0) and a metallic one for the bulk (BG = 0). For values In between, covalent contributions arise and a decrease of BG with increasing cluster size is observed.

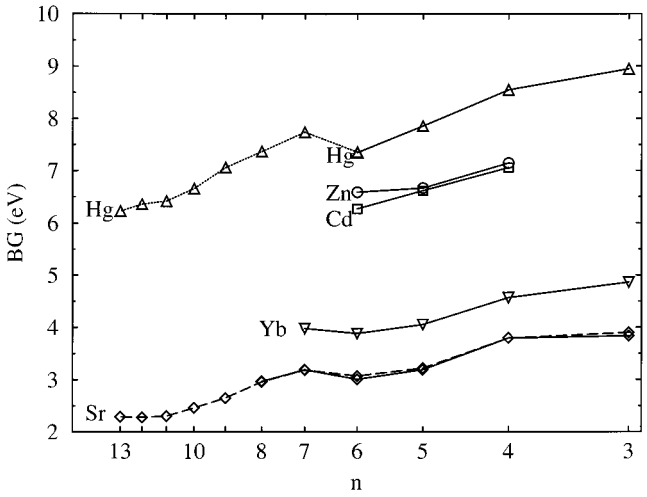

Figure 5. The band gap BG = IP − EA (eV) for Sr, Yb, and the corresponding group 12 clusters. The symbols have the same meaning as in Figure 2. The dotted line for Hg denotes PDMC results from ref 4.

Therefore BG is also a suitable quantitative global measure of covalent contributions to bonding in clusters. It will be shown below in the analysis using ELF that the local bonding characteristics within a cluster may depend on the environment of the atom under consideration. BG significantly decreases from Sr_3 to Sr_{13} by 1.54 eV and therefore the overall covalent contributions to bonding considerably increase. However, the BG is still 2.29 eV for Sr_{13} and there is a long way to go to reach metallic behavior. It should be noted that the DFT calculations of Qureshi and Kumar[15] yield a band gap below 0.1 eV for Sr_{13}. Experimental data is needed to decide which approach yields a more realistic picture.

3.4. Bonding Analysis Using ELF. The properties studied so far are global in character and their evolution with increasing cluster size allows one to draw conclusions with respect to bonding in the systems as a whole. However, even in larger elemental clusters one may have different bonding situations depending on the position of the atoms in the cluster. One of the major advantages of ELF is that it can directly reveal the local character of bonding between two atoms. In general a low-valued saddle point exists in the ELF values between two atoms for a pure van der Waals interactions, while a high-valued maximum occurs for typical covalent interactions, i.e., one can easily distinguish between van der Waals and covalent interactions. Therefore ELF is especially suitable to investigate the transition between different types of bonding.

Figure 6a shows ELF for Sr_2. A maximum of ELF = 0.67 between the two atoms is observed, which is qualitatively different from the group 12 and Yb homonuclear dimers where saddle points were present (ELF = 0.05, 0.05, 0.06, and 0.29 for Zn_2, Cd_2, Hg_2, and Yb_2, respectively). This is a clear indication of covalent bonding contributions in Sr_2, and to a lesser extent in Yb_2, whereas the group 12 dimers are still dominated by van der Waals interactions. Qualitatively a similar conclusion was obtained by a completely independent method, i.e., the analysis of charge fluctuations (Figure 1]), however quantitatively the differences in the character of bonding appear to be more dramatic for ELF. An interesting problem is to analyze which atomic orbitals (p, d) are mainly responsible for the covalent bonding contributions in Sr_2. Using a (5s5p6d) basis set the maximum ELF value is 0.61, i.e., 10% lower than for the full (5s5p6d3f1g) basis set. The reduced (5s5p) and (5s6d) basis sets yield values of 0.39 (Figure 6b) and 0.38 (Figure 6c), respectively, indicating an essentially equal importance of p and d functions. The significant increase of the maximum ELF value between the atoms is accompanied by an increase of the electron density between the atoms as it is obvious from the shape of the contour lines in Figure 6a−c. In contrast to the previous analysis of the structure and the cohesive energy we calculate ELF here and in the following for the equilibrium structure determined with the best basis set at the CCSD(T) level.

Even stronger covalent bonding occurs for Sr_3, e.g., as it is visualized by the red-white interatomic region of high ELF values in Figure 6d, which also exhibits a local maximum (ELF = 0.89). Similar to Yb_3, the maximum somewhat deviates from the interatomic axis. This behavior is well-known from covalently bound systems with high strain, e.g., carbosilane,[35] where the possible bonding angles of the sp^n hybridization do not agree with those dictated by the number and positions of the neighbor atoms. Again, using the reduced (5s5p6d) basis set lowers the ELF maximum by nearly 10% (ELF = 0.81), and p and d orbitals contribute equally. The maximum ELF values are 0.58 (Figure 6e) and 0.56 (Figure 6f) for (5s5p) and (5s6d), respectively.

The situation is quite similar for Sr_4 (Figure 6g). Note that again the position of the 3D maximum is not exactly in the depicted plane containing three atoms. The maximum ELF values are 0.77, 0.60, and 0.57 for (5s5p6d), (5s5p), and (5s6d), respectively. Similarly, for Sr_5 (Figure 6h) ELF values of 0.79, 0.68, and 0.62 are observed. Summing results obtained for Sr_2 to Sr_5, the analysis of bonding by means of ELF in connection with various truncated basis sets is in line with the corresponding findings for structures and cohesive energies. Both p and d orbitals are of significant importance in Sr clusters.

To compare the covalent contributions of p and d orbitals with those in Yb clusters, ELF pictures with and without d functions have been produced for Sr_5 (Figure 6h and 6i) and Yb_5 (Figure 6j and 6k). For comparison Zn_5, exhibiting a significantly lower covalency, is also shown (Figure 6l). It should be noted that in contrast to Sr and Yb clusters the influence of d functions on the ELF pictures of Zn_5 and other group 12 clusters is almost negligible.

In the case of the bicapped tetrahedral structure of Sr_6, Figure 6m shows a plane which includes the two cap atoms and two tetrahedral atoms. The covalency within the tetrahedral skeleton (ELF = 0.73) is slightly lower than in the corresponding Sr_4 cluster (ELF = 0.81), although the bond lengths are nearly identical (4.02 vs 4.01 Å). However, the covalent interactions between cap atoms and tetrahedral atoms (ELF = 0.89) are slightly stronger despite the larger bond length (4.12 Å).

Two especially interesting cases are ELF pictures of the pentagonal bipyramidal Sr_7 and the icosahedral Sr_{13} structures. The two axial atoms of Sr_7 possess the shortest bond distance among all the clusters considered in this work (3.88 Å). Figure 6n shows a region of high ELF values squeezed together between the cores of the axial atoms. As already mentioned, the short distance between the two axial atoms of Sr_7 results from the fact that there are five axial−equatorial interactions for each axial atom. An ELF picture for Sr_{13} is shown in Figure 6o. The plane includes the center and four surface atoms. Regions with high ELF indicating a high covalency (ELF = 0.77) are visible between the center and the other two adjacent surface atoms.

4. Conclusions

Strontium clusters with up to 13 atoms were investigated by quantum chemical ab initio techniques using a scalar-relativistic pseudopotential, a core-polarization potential, large valence basis

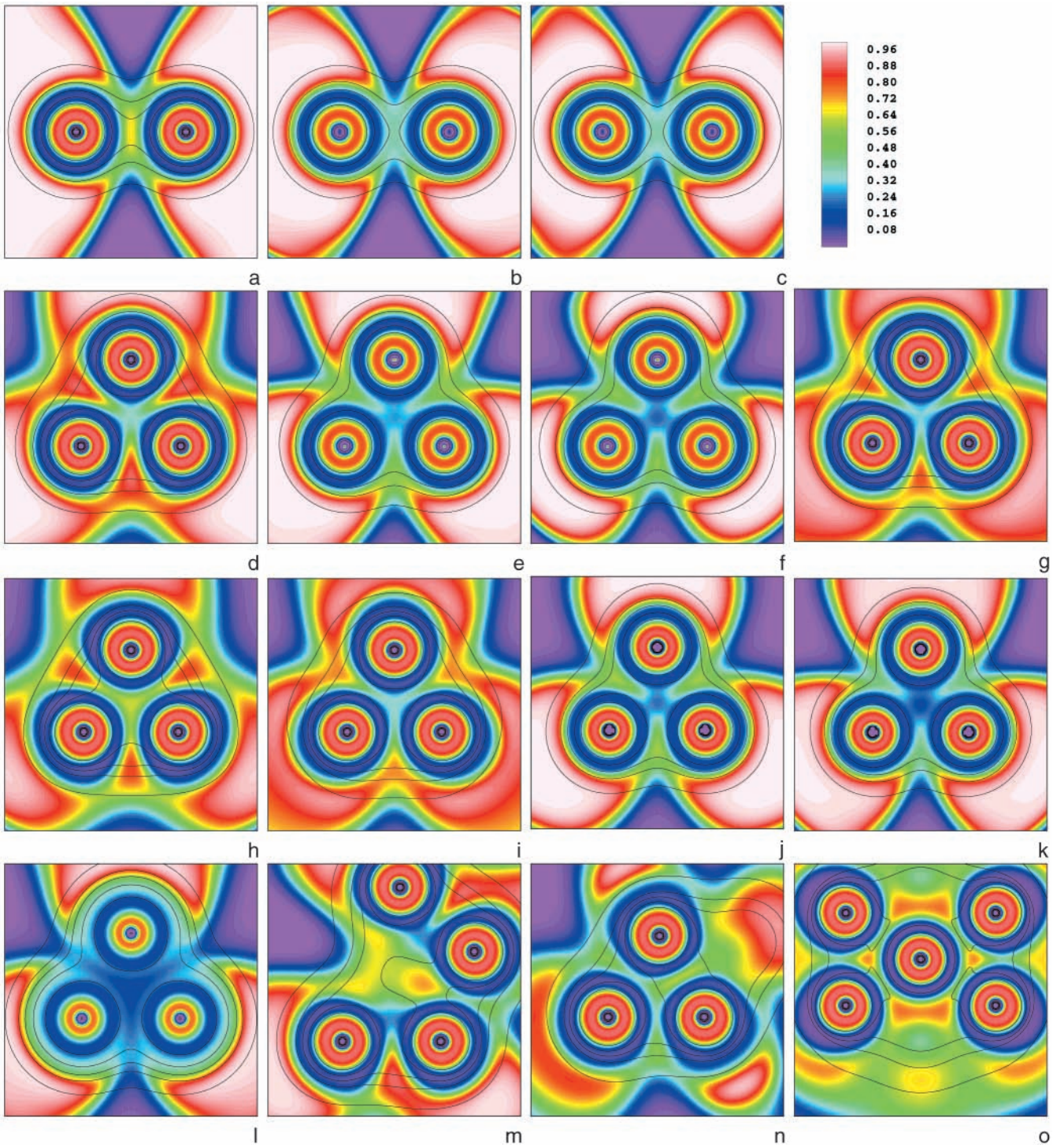

Figure 6. 2D plots of ELF. The ELF values are encoded by colors and overlayed by contour lines of the electron densities. The outmost contour line of 0.001 au indicates the approximate size of the cluster. The plots refer to PP(10) calculations unless otherwise noted. (a,b,c) Sr_2 with full, sp, and sd basis sets; (d,e,f) equilateral triangular structure of Sr_3 with full, sp, and sd basis sets; (g) surface of the tetrahedral structure of Sr_4; (h,i) equatorial plane of the trigonal bipyramidal structure of Sr_5 with and without d orbitals; (j,k) as (h,i) but for Yb_5; (l) as (h) but for Zn_5 (PP(2)+CPP calculation, pseudo-core orbitals added; (m) section through two cap atoms and two tetrahedral atoms of the bicapped tetrahedral structure of Sr_6; (n) section through two axial and one equatorial atom of the pentagonal bipyramidal structure of Sr_7; (o) section through the center and other four atoms of Sr_{13}.

sets and a coupled-cluster correlation treatment. In agreement with experimental evidence Sr_4 and Sr_7 have been found to be especially stable, whereas Sr_{13} is not. The analysis of global properties such as the cohesive energy per atom or the band gap defined as the difference between ionization potential and electron affinity, as well as the local information provided by the electron localization function, indicates that small to medium-sized Sr clusters have a stronger covalent bonding contribution than the previously investigated Yb clusters. In qualitative agreement to previous conclusions of other authors based on calculations using the local density approximation, the 4d orbitals appear to be at least equally important to the 5p orbitals for bonding in Sr clusters. These findings are supported by a bonding analysis using the electron localization function for the Hartree−Fock wave functions at the equilibrium structures determined by correlated calculations.

Acknowledgment. The authors thank F. Schautz, Dresden, for critically reading the manuscript as well as for his assistance in the production of the ELF pictures. The support of Prof. P. Fulde, Dresden, is gratefully acknowledged.

References and Notes

(1) Pastor, G. M.; Bennemann, K. H. In *Clusters of Atoms and Molecules*; Haberland, H., Ed.; Springer: Berlin, 1994; Vol. 1, p 86.

(2) de Heer, W. A. *Rev. Mod. Phys.* **1993**, *65*, 611.

(3) Dolg, M.; Flad, H.-J. *J. Phys. Chem.* **1996**, *100*, 6147.

(4) Dolg, M.; Flad, H.-J. *Mol. Phys.* **1997**, *91*, 815.

(5) Flad, H.-J.; Schautz, F.; Wang, Y.; Dolg, M.; Savin A. *Eur. Phys. J. D* **1999**, *6*, 243.

(6) Wang, Y.; Schautz, F.; Flad, H.-J.; Dolg, M. *J. Phys. Chem. A* **1999**, *103*, 5091.

(7) Wang, Y.; Dolg, M. *Theor. Chem. Acc.* **1998**, *100*, 124.

(8) Wang, Y.; Flad, H.-J.; Dolg, M. *Phys. Rev. B* **2000**, *61*, 2362.

(9) Dugourd, P.; Chevaleyre, J.; Bordas, C.; Broyer, M. *Chem. Phys. Lett.* **1992**, *193*, 539.

(10) Bréchignac, C. *private communication cited in ref 15.*

(11) Hearn, J. E.; Johnston, R. L. *J. Chem. Phys.* **1997**, *107*, 4674.

(12) Boutassetta, N.; Allouche, A. R.; Aubert-Frécon, M. *Phys. Rev. A* **1996**, *53*, 3845.

(13) Jones, R. O. *J. Chem. Phys.* **1979**, *71*, 1300.

(14) Ortiz, G.; Ballone, P. *Phys. Rev. B* **1991**, *43*, 6376.

(15) Qureshi, T.; Kumar, V. *d-Electron Induced Icosahedral Growth in Strontium Clusters*; Condensed Matter E-Print Server at http://babbage.sissa.it/archive/cond-mat/9806, manuscript 167.

(16) Flad, H.-J.; Dolg, M. *J. Phys. Chem.* **1996**, *100*, 6152.

(17) Kaupp, M.; Schleyer, P. v. R.; Stoll, H.; Preuss, H. *J. Chem. Phys.* **1991**, *94*, 1360.

(18) Fuentealba, P.; v. Szentpaly, L.; Preuss, H.; Stoll, H.; *J. Phys. B* **1985**, *18*, 1287.

(19) MOLPRO is a package of ab initio programs written by H.-J. Werner and P. J. Knowles, with contributions from J. Almlöf, R. D. Amos, M. J. O. Deegan, S. T. Elbert, C. Hampel, W. Meyer, A. Nicklass, K. Peterson, R. M. Pitzer, A. J. Stone, and P. R. Taylor; Werner, H.-J.; Knowles, P. J. *Theor. Chim. Acta* **1990**, *78*, 175; Hampel, C.; Peterson, K.; Werner, H.-J. *Chem. Phys. Lett.* **1992**, *190*, 1.

(20) Becke, A. D.; Edgecombe, K. E. *J. Chem. Phys.* **1990**, *92*, 5397.

(21) Savin, A.; Nesper, R.; Wengert S.; Fässler, T. F. *Angew. Chem., Int. Ed. Engl.* **1997**, *36*, 1808, and references therein.

(22) Schautz, F.; program for the evaluation of ELF.

(23) Fulde P. *Electron Correlations in Molecules and Solids*, 2nd ed.; Springer: Berlin, 1993.

(24) Schwerdtfeger, P.; Fischer, T.; Dolg, M.; Igel-Mann, G.; Nicklass, A.; Stoll, H.; Haaland, A. *J. Chem. Phys.* **1995**, *102*, 2050.

(25) Leininger, T.; Nicklass, A.; Stoll, H.; Dolg, M.; Schwerdtfeger, P. *J. Chem. Phys.* **1996**, *105*, 1052.

(26) Leininger, T.; Nicklass, A.; Küchle, W.; Stoll, H.; Dolg, M.; Bergner, A. *Chem. Phys. Lett.* **1996**, *255*, 274.

(27) Schautz, F.; Flad, H.-J.; Dolg, M. *Theor. Chem. Acc.* **1998**, *99*, 231.

(28) Gerber, G.; Möller; R., Schneider, H. *J. Chem. Phys.* **1984**, *81*, 1538.

(29) Yu, M.; Dolg, M. *Chem. Phys. Lett.* **1997**, *273*, 329.

(30) Kawai, R.; Weare J. H. *Phys. Rev. Lett.* **1990**, *65*, 80.

(31) Boutou, V.; Allouche, A. R.; Spiegelmann, F.; Chevaleyre, J.; Aubert Frécon, M. *Eur. Phys. J. D* **1998**, *2*, 63.

(32) Kumar, V.; Car, R. *Z. Phys. D.* **1991**, *19*, 177.

(33) Busani, R.; Folkers, M.; Cheshnovsky, O. *Phys. Rev. Lett.* **1998**, *81*, 3836.

(34) Roggen, I.; Amlöf, J. *Int. J. Quantum Chem.* **1996**, *60*, 453.

(35) Savin, A.; Flad, H.-J.; Flad, J.; Preuss, H.; von Schnering, H. G. *Angew. Chem.* **1992**, *104*, 185; *Angew. Chem., Int. Ed. Engl.* **1992**, *31*, 187.

(36) Schwartz, H. L.; Miller, T. M.; Bederson B. *Phys. Rev. A* **1974**, *10*, 1924.

(37) Hyman, H. A. *J. Chem. Phys.* **1974**, *61*, 4063.